Mechanical instabilities of homogeneous crystals

Jinghan Wang, Ju Li, and Sidney Yip
Department of Nuclear Engineering, Massachusetts Institute of Technology, Cambridge, Massachusetts 02139

Simon Phillpot and Dieter Wolf
Materials Science Division, Argonne National Laboratory, Argonne, Illinois 60439
(Received 24 May 1995)

Elastic stability criteria are derived for homogeneous lattices under arbitrary but uniform external load. These conditions depend explicitly on the applied stress and reduce, in the limit of vanishing load, to the criteria due to Born, involving only the elastic constants of the crystal. By demonstrating the validity of our results through a comparison of the analysis of an fcc lattice under hydrostatic tension with direct molecular-dynamics simulation, we show that crystal stability under stress (ideal strength) is not a question only of material property, and that even qualitative predictions require the inclusion of the effects of applied stress. General implications of our findings, as well as relevance to stability phenomena in melting, polymorphism, crack nucleation, and solid-state amorphization, are discussed.

I. INTRODUCTION

The fundamental basis for understanding the mechanical stability of the solid state lies in the formulation of stability criteria, a set of conditions which specify the critical level of external stress or internal strain under which a homogeneous lattice, without defects of any kind, becomes structurally unstable. Lattice stability is not only one of the most central issues in elasticity, it is also an essential consideration in the analysis of structural responses in solids, ranging from polymorphism, amorphization, and melting to fracture. It may seem surprising, therefore, that despite the recognized importance of assessing crystal stability, the question of the proper formulation of stability criteria at finite load remains an open issue.

The systematic analysis of lattice stability is generally attributed to Born,[1] who showed that by expanding the internal energy of a crystal in a power series in the strain and by requiring convexity (positivity) of the energy, one obtains stability criteria in the form of a set of conditions on the elastic constants appropriate to the crystal. While Born's results are well known,[2] the fact that they are valid only under conditions of zero load has not always been appreciated.[3–5] In a critical discussion of instability analysis of homogeneous lattices, Hill[6] has pointed out certain confusion in the literature where the Born criteria had been used to determine theoretical strengths of perfect crystals.[3–5] The problem lies in that when the crystal is under load, the first-order changes in the surface tractions in an incremental deformation have to be specified, as both the external work done and the change in the internal energy are evaluated to second order.[6] Stability thus can be regarded in the sense of a mechanical test or as an intrinsic property of the material. In the former, the loading is frame dependent and the work is affected by rotation, whereas in the latter one imagines that the loading "follows" the material during deformation and is therefore frame independent. Without concluding which view is more physically meaningful, Hill stressed the relativity aspect of the stability concept, namely, in a crystal under load, convexity of the internal energy is coordinate dependent.[6] In a following series of comprehensive theoretical and computational studies, Hill and Milstein showed that different choices of strain measures lead to different domains of stability.[7–11]

The purpose of this paper is to present a method for analyzing the onset of instabilities in homogeneous lattices under critical loading. By formulating a Gibbs integral which combines the change in the Helmholtz free energy and the external work done during deformation (in analogy with the Gibbs free energy), we derive stability criteria in which the elastic stiffness coefficients B appear in place of the elastic constants C. Because B depends explicitly on the applied stress and therefore does not have Cauchy symmetry, it is necessary to define stability strictly in terms of the symmetrized form of B. Nevertheless, we can give arguments which indicate that stability criteria involving only B may be quite robust. Next we consider the case of a cubic lattice under hydrostatic loading to obtain predictions of critical strain and mode of deformation, along with numerical results based on an explicit atomistic model. The predictions are tested by molecular-dynamics simulations, carried out at constant applied stress, in which the onset of structural instability is explicitly observed and the mode of instability is determined. In this direct manner we demonstrate the validity of our stability criteria at finite load.

In the present approach we do not deal directly with the Gibbs integral which is dependent on the deformation path in most cases. Instead we interpret it as the result of path integration in a field of driving forces, and obtain the stability criteria from the first-order expansion of this force field around equilibrium position, in terms of the strain. The elastic stiffness tensor then appears as the sum of the elastic constant tensor and another fourth-rank tensor (second-rank in deformation space) which depends solely on the applied load. Since the latter has symmetry determined by the applied load, this means the response of the lattice is no longer a purely intrinsic property of the material system. In the limit of vanishing load, the present results reduce to the stability criteria derived by Born.[1,2]

0163-1829/95/52(17)/12627(9)/$06.00

The paper is organized as follows. Derivation of stability criteria is discussed in Sec. II, where one can see clearly the connection to Born's results. In Sec. III we specialize to the case of a cubic lattice and hydrostatic loading, a particularly simple situation which is nevertheless sufficient to illustrate the importance of the explicit role of the external stress. In Sec. IV we discuss first numerical evaluations of the elastic stiffness coefficients necessary for the prediction of the critical strain at which an fcc lattice becomes unstable. Then molecular-dynamics simulation results are presented to show the effectiveness of the instability criteria. We conclude in Sec. V by commenting on the fundamental role that elastic instability can play in structural responses to stress or temperature.

II. LATTICE STABILITY AT FINITE LOADING

Consider a perfect lattice undergoing homogeneous deformation under an applied load. In response to the load, the system configuration changes from X to $Y=JX$, where J is the deformation gradient or the Jacobian matrix.[12] The associated Lagrangian strain tensor is defined as

$$\eta=(1/2)(J^TJ-1). \tag{2.1}$$

All homogeneous deformations can be described by the movement of a configuration variable in *deformation space*, in general a nine-dimensional space with origin at an arbitrarily chosen reference state X. In this space any configuration point can be uniquely represented by the transformation matrix J (relative to X). Moreover, if there exists particular constraints which allow us to uniquely determine J from η, then deformation space becomes six-dimensional, which we call *unique* to denote the fact that any configuration can be specified in terms of η instead of J. As an example, in the Parrinello-Rahman method for performing atomistic simulation at constant stress,[13] J is usually constrained to be symmetric. Because J in this case can then be uniquely determined from η through the equation

$$J=\sqrt{1+2\eta}=1+\eta-(1/2)\eta^2+\cdots, \tag{2.2}$$

we will refer to such a deformation space as *symmetric*. (Notice that there can be other unique deformation spaces. For instance, we can constrain J to be always upper triangular, so it has only 6 degrees of freedom which is also uniquely determined by η.) The opposite of unique is the *general* case which we will discuss elsewhere. For the present deformation under an applied load the change in the Helmholtz free energy, a quantity which is rotationally invariant, and therefore only a function of η, can be always expanded into a power series of η,

$$\begin{aligned}\Delta F&=F(X,\eta)-F(X,0)\\&=V(X)[t(X)\eta+(1/2)C(X)\eta\eta+\cdots].\end{aligned} \tag{2.3}$$

In (2.3) we have the conventional definitions of the thermodynamic stress and second-order elastic constant tensor,

$$t_{ij}(X)=\frac{1}{V(X)}\hat{S}_2\left(\left.\frac{\partial F}{\partial\eta_{ij}}\right|_{\eta=0}\right), \tag{2.4}$$

$$C_{ijkl}(X)=\frac{1}{V(X)}\hat{S}_4\left(\left.\frac{\partial^2 F}{\partial\eta_{ij}\partial\eta_{kl}}\right|_{\eta=0}\right), \tag{2.5}$$

where $\hat{S}_n$ is the nth rank symmetrization operator,

$$\begin{aligned}\hat{S}_2(G_{ij})&=(G_{ij}+G_{ji})/2,\\ \hat{S}_4(G_{ijkl})&=(G_{ijkl}+G_{jikl}+G_{ijlk}+G_{jilk})/4,\end{aligned} \tag{2.6}$$

etc.

For the work that will be done by an external stress τ, we let Y be any point on the deformation path and consider a virtual move near Y along the path, i.e., $J\rightarrow J+\delta J$. We have in mind a deformation space with configuration X as the origin and the reference state for η. The incremental work done is then given by the surface integral

$$\begin{aligned}\delta W&=\oint_S\tau_{ij}n_j\cdot\delta u_i dS=\int_Y\nabla\cdot(\tau\delta u)dV=V(Y)\tau_{ij}\frac{\partial\delta u_i}{\partial Y_j}\\&=V(Y)\frac{\tau_{ij}}{2}\left(\frac{\partial\delta u_i}{\partial Y_j}+\frac{\partial\delta u_j}{\partial Y_i}\right).\end{aligned} \tag{2.7}$$

Here δu is the virtual displacement on the surface. Making use of the fact that $\delta u=(\delta J)X=\delta J\cdot J^{-1}Y$, which leads to

$$\delta W=V(Y)\frac{\tau_{ij}}{2}(\delta J\cdot J^{-1}+J^{-T}\cdot\delta J^T)_{ij}, \tag{2.8}$$

and the fact that the differential of (2.1) is

$$\delta\eta=(1/2)[J^T\delta J+(\delta J^T)J], \tag{2.9}$$

or

$$J^{-T}\delta\eta J^{-1}=(1/2)[\delta J\cdot J^{-1}+J^{-T}\cdot\delta J^T], \tag{2.10}$$

we obtain for the incremental (differential) work,

$$\delta W=V(Y)\mathrm{Tr}(J^{-1}\tau J^{-T}\delta\eta). \tag{2.11}$$

The work done over the deformation path l is therefore

$$\Delta W(l)=\int_l V(Y)\mathrm{Tr}(J^{-1}\tau J^{-T}d\eta). \tag{2.12}$$

To examine the system stability at configuration X we consider the difference between the increase in Helmholtz free energy and the work done by external stress,

$$\Delta G(Y,l)=\Delta F(X,\eta)-\Delta W(l)=\int_l\boldsymbol{g}(Y)\cdot d\boldsymbol{\eta} \tag{2.13}$$

with

$$\boldsymbol{g}(Y)=\frac{\partial F}{\partial\eta}-V(Y)J^{-1}\tau J^{-T}. \tag{2.14}$$

We define ΔG to be the *Gibbs integral* in analogy with the Gibbs free energy which is the appropriate thermodynamic potential in the (NTP) ensemble. However, it is important to point out that ΔG might be dependent on the deformation path in this more general case of constant stress condition (to be shown later). This means that this quantity is not a true thermodynamic potential to which one can apply

the usual stability analysis. Nevertheless, we can identify $-\boldsymbol{g}(Y)$ as the *Gibbs driving force* and focus on its property as a force field in deformation space to formulate a stability analysis.

The spirit of our analysis here may be compared to a virtual work argument. Stability of a lattice under load may be determined by imagining the lattice undergoing a virtual displacement, with the applied stress held constant. Then one asks whether the work that would be done by the applied load exceeds that absorbed as an increase in internal energy. If this situation obtains, then an excess energy would be available to cause the displacement to grow, and the lattice would be unstable.

From now on we will analyze stability behavior in *symmetric* deformation space. Since there is a one-to-one correspondence between η and J, the space is six dimensional and all related second-rank tensors (strains and stresses) can be treated as vectors in this space (taking the trace between two matrices is like taking an inner product between two vectors). On the basis of (2.13) we can interpret $-\boldsymbol{g}(Y)$ as the *direction of steepest descent* at configuration Y, and regard it as the most plausible way for the system to evolve at that point, at least for quasistatic processes. To show that $\boldsymbol{g}(Y)$ has the property of a force field, let us assume the condition for equilibrium at X to be the requirement that no first-order change in ΔG occurs for any small variation about X. This can only be satisfied by the condition

$$g_{ij}(X)=\left[\frac{\partial F}{\partial \eta_{ij}}-V(Y)(J^{-1}\tau J^{-T})_{ij}\right]_{J=1}$$
$$=V(X)[t_{ij}(X)-\tau_{ij}]=0, \tag{2.15}$$

or

$$t_{ij}(X)=\tau_{ij}\ ; \tag{2.16}$$

thus, the condition for mechanical equilibrium is, as expected, the equality between external load τ_{ij} and the internal stress $t_{ij}(X)$.

Suppose the system, initially at equilibrium at X under stress $\tau(\boldsymbol{g}(X)=0)$, is perturbed to configuration Y with corresponding strain η. In view of (2.14) the first-order expansion for $\boldsymbol{g}(Y)$ becomes

$$g_{ij}(Y)=g_{ij}(\eta)=V(X)B_{ijkl}\eta_{kl}+\cdots, \tag{2.17}$$

where

$$B_{ijkl}=C_{ijkl}-\frac{\partial(\det|J|J^{-1}_{im}\tau_{mn}J^{-1}_{nj})}{\partial\eta_{kl}}\Big|_{\eta=0,\ J=1}. \tag{2.18}$$

Since

$$J^{-1}=\frac{1}{\sqrt{1+2\eta}}=1-\eta+\cdots, \tag{2.19}$$

$$\det|J|=1+\mathrm{Tr}(\eta)+\cdots, \tag{2.20}$$

(2.18) can be evaluated to give

$$B_{ijkl}=C_{ijkl}-\delta_{kl}\tau_{ij}+\delta_{ik}\tau_{jl}+\delta_{jl}\tau_{ik}. \tag{2.21}$$

Because η_{ij} and $\eta_{ji}(\eta_{kl}$ and $\eta_{lk})$ are not separate variables, we need to symmetrize with respect to the interchange of indices $(i\leftrightarrow j)$ and $(k\leftrightarrow l)$. Thus,

$$B_{ijkl}=C_{ijkl}+(1/2)(\delta_{ik}\tau_{jl}+\delta_{jk}\tau_{il}+\delta_{il}\tau_{jk}+\delta_{jl}\tau_{ik}-2\delta_{kl}\tau_{ij}). \tag{2.22}$$

Equation (2.22) is the expression defining the elastic stiffness coefficient B.[14] We can see that B does not possess $(ij)\leftrightarrow(kl)$ symmetry, so ΔG is path dependent in general, unless the applied load is hydrostatic, $\tau_{ij}\propto\delta_{ij}$.

The physical implication of (2.17) is that in deformation space the shape of the force field around the origin is described by the "second-rank tensor" B. Consider now the following inner product:

$$\lambda=\boldsymbol{\eta}\cdot B\,\boldsymbol{\eta}. \tag{2.23}$$

Because $-B\,\boldsymbol{\eta}$ should be the most probable direction for action, if we can show that $\lambda>0$ for any η near the origin, then it means the system is always moving toward the origin, no matter how it is initially perturbed. This means the system is stable. On the other hand, if one can find an $\boldsymbol{\eta}$ for which $\lambda<0$, then there exists a path which will lead the system to instability. Given that B is in general asymmetric, the stability of B is governed by its symmetrized counterpart,

$$A=(1/2)(B^T+B), \tag{2.24}$$

because

$$\lambda=\eta^T B_\eta=(1/2)\,\eta^T(B^T+B)\,\eta \tag{2.25}$$

for any column vector $\boldsymbol{\eta}$. The stability criterion is then the requirement that all the eigenvalues of A be positive. Stated another way, the system becomes unstable when

$$\det|A|=0 \tag{2.26}$$

for the first time.

We can also propose an equivalent "free energy" argument. We had been purposely avoiding the term "free energy" because ΔG might depend on path as well as the final state. But suppose we can stipulate a path for every final position beforehand, then

$$\Delta G(Z,l)=\Delta G(Z,l(Z))=\Delta G^*(Z) \tag{2.27}$$

again, and the problem is superficially solved. For convenience we will define the path for every point in space to be the straight line between it and the origin, and the corresponding criterion can be simply stated as "The system is stable if and only if $\Delta G^*(Z)>0$ for any Z near the origin."

It is easy to show that this criterion is totally equivalent to (2.26) because a straight path integral of a linearly dependent function $\boldsymbol{g}(\boldsymbol{\eta})=B\,\boldsymbol{\eta}$ will simply give us

$$\Delta G^*(\boldsymbol{\eta})=(1/2)\,\boldsymbol{\eta}\cdot B\,\boldsymbol{\eta}=(1/2)\,\boldsymbol{\eta}\cdot A\,\boldsymbol{\eta}, \tag{2.28}$$

as long as the first-order expansion is valid.

We can easily show that when

$$\det|B|=0 \tag{2.29}$$

the system is already unstable. However, this is a "weaker" criterion than (2.26) because it cannot predict definitely the

incipient instability mode. Yet it can turn out that some modes predicted by (2.29) are identical to the prediction of (2.26) due to reasons of underlying symmetry, and if the incipient mode is among those common ones, then the two criteria are equivalent as far as incipient instability is concerned. One example is the uniaxial tension case, where the $C_{22}=C_{23}$ mode is predicted by both (2.26) and (2.29), and this happens to be the incipient instability mode found in the simulation studies we have carried out. Thus it appears that the "B criteria" are quite robust.

One should also keep in mind that results from (2.17) to (2.29) are only for symmetric deformation space, which is the dominant situation in computer simulation. Stability criteria for general deformation space have been derived and will be discussed in a future publication.

III. STABILITY CRITERIA FOR A CUBIC LATTICE

To exhibit explicitly instability criteria for a particular lattice type and applied loading, we consider a cubic lattice under hydrostatic pressure

$$\tau_{ij}=-P\delta_{ij}. \tag{3.1}$$

In this case B is symmetric, and there is genuine Gibbs free energy. We follow the convention that inward pressure is positive while inward stress is negative ($P<0$ for tension). Given (3.1) one finds from (2.22) that the nonzero elements of the stiffness coefficients are

$$\begin{aligned} &B_{11}=B_{22}=B_{33}=C_{11}-P,\\ &B_{12}=B_{21}=B_{13}=C_{12}+P,\\ &B_{44}=B_{55}=B_{66}=4(C_{44}-P). \end{aligned} \tag{3.2}$$

In the present case of volumetric deformation the stiffness coefficients and the elastic constants have the same symmetry. Inserting these elements into (2.29) gives three instability criteria and corresponding eigenmodes of deformation,

$$C_{11}+2C_{12}+P=0, \quad (1,1,1,0,0,0)\,\delta\eta \tag{3.3}$$

$$C_{11}-C_{12}-2P=0, \quad \begin{matrix}(\delta\eta_{xx},\delta\eta_{yy},\delta\eta_{zz},0,0,0)\\ \delta\eta_{xx}+\delta\eta_{yy}+\delta\eta_{zz}=0\end{matrix} \tag{3.4}$$

$$C_{44}-P=0, \quad (0,0,0,\delta\eta_{yz},0,0). \tag{3.5}$$

These results have straightforward interpretations. The first criterion clearly has to do with volumetric deformation, as indicated by its eigenmode. Also, with $C_{11}+2C_{12}=3B_T$, where B_T is the isothermal bulk modulus, we see that for (3.3) to be satisfied, P would have to be negative. Thus, the nature of this instability is lattice decohesion by pure dilatation. Since it involves the vanishing of the bulk modulus, we will refer to it as the *spinodal* instability. The second instability, (3.4) involves symmetry breaking (bifurcation) with volume conservation; the vanishing modulus here may be identified as the tetragonal shear, $G'=(C_{11}-C_{12})/2$. We will refer to this as the *Born* instability. The third instability is the simple shear along one of the symmetry directions, with volume conservation; the modulus here is $G=C_{44}$.

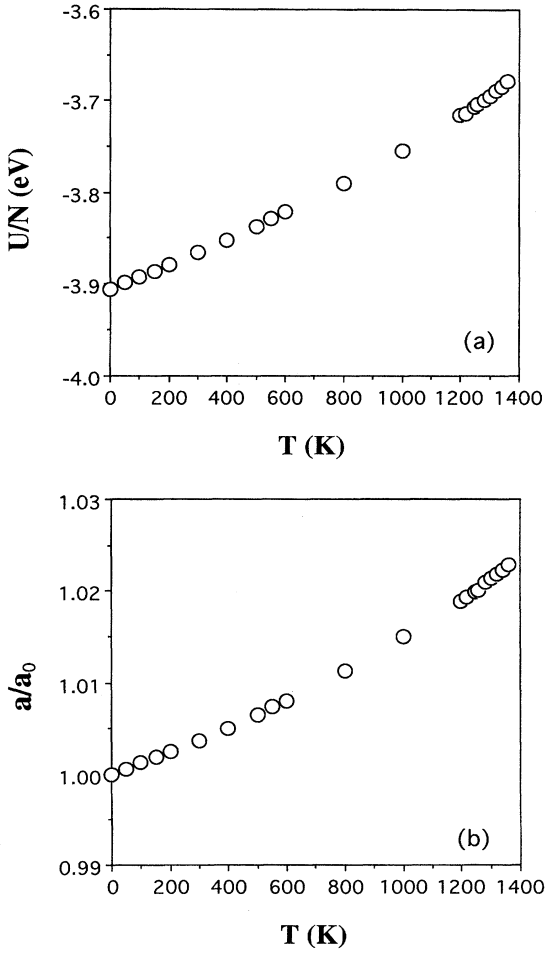

FIG. 1. Potential energy per atom (a) and lattice parameter (b) of EAM (Au) model at various temperatures and zero pressure; a_0 is the lattice parameter at 0 K.

IV. DILATATION-INDUCED INSTABILITY

To investigate the instability induced by an applied hydrostatic stress we perform molecular-dynamics simulation using an interatomic potential model of the embedded-atom type (EAM) developed for Au.[15] (The particular choice of the potential has no special significance here since we are interested only in the generic features of the results.) The simulation cell is cubic and contains $N=504$ atoms, arranged in an fcc structure with periodic border conditions imposed in the manner of Parrinello and Rahman.[13] A series of isothermal-isostress simulations are carried out at several temperatures, each over a range of applied tension up to and beyond the point of instability. At each temperature the atomic trajectories generated are used to compute the elastic constants C_{ij} at the current state of tension using appropriate fluctuation formulas.[16] Having determined the elastic constants in this manner, the elastic stiffness coefficients are obtained through (2.22).

Since molecular dynamics allows us to examine not only

the system stability at various levels of applied stress, but also the effects of temperature, we show first in Fig. 1 how our simulation model behaves under isobaric ($P=0$) heating. The variations of the potential energy and the lattice parameter at zero pressure are those characteristic of a crystal undergoing normal thermal expansion; the lattice expands as temperature increases, while the potential energy also increases because thermal motions cause the instantaneous system configurations to be relatively more disordered. The simulation data for both quantities can be fitted well to a quadratic expansion in the temperature. We will henceforth regard the lattice parameter ratio a/a_0, where a_0 is the equilibrium (minimum energy) value at zero temperature, as a convenient measure of lattice strain η. Notice that so long as the system is stable, there is a one-to-one correspondence between η and T [Fig. 1(b)]. Thus, at finite temperature the lattice is under strain even though the system is under zero load.

We have determined the variations of the elastic constants and elastic stiffness coefficients with hydrostatic loading at several temperatures, 200, 500, 800, 1000, and 1200 K. Since the stability criteria are given in terms of elastic moduli, it is more relevant to examine their behavior under load. We first define the bulk modulus and the two shear moduli,

$$B_T=(\tfrac{1}{3})(C_{11}+2C_{12}), \tag{4.1}$$

$$G'=(\tfrac{1}{2})(C_{11}-C_{12}), \tag{4.2}$$

$$G=4C_{44}. \tag{4.3}$$

Next we introduce their extensions to finite hydrostatic loading,

$$B_T(\tau)=(\tfrac{1}{3})(B_{11}+2B_{12})=(\tfrac{1}{3})(C_{11}+2C_{12}+P), \tag{4.4}$$

$$G'(\tau)=(\tfrac{1}{2})(B_{11}-B_{12})=(\tfrac{1}{2})(C_{11}-C_{12}-2P), \tag{4.5}$$

$$G(\tau)=B_{44}=4(C_{44}-P). \tag{4.6}$$

In the limit of zero load (4.4)–(4.6) obviously reduce to (4.1) and (4.3), whereas at finite load, the two sets of moduli are both well defined and clearly differ from each other. In contrast to the conventional stability criteria which require that (4.1)–(4.3) be positive, the stability criteria derived in Sec. III require instead (4.4)–(4.6) to be positive.

In Fig. 2 we show how the two sets of moduli vary with strain at a relatively low temperature of 500 K. These results are obtained by imposing a certain hydrostatic load on the simulation cell and allowing the system to come to equilibrium. After equilibrium is reached, long simulation runs are made to collect trajectory data for the calculation of the three elastic constants, C_{11}, C_{12} and C_{44}, using fluctuation formulas[16] at various levels of applied load. Comparing the conventional elastic moduli defined in (4.1)–(4.3) with their counterparts defined in terms of elastic stiffness coefficients, we see the effect of the applied stress [see (2.22)] is most pronounced in the tetragonal shear modulus G', less so in G, and even less in B_T. The significance of Fig 2 is that on the basis of (3.3)–(3.5) one would predict the lattice to undergo decohesion at a strain of 1.060, while the conventional criteria would predict an instability caused by the vanishing of G' at a strain of 1.025. These two predictions are sufficiently different that a direct simulation of the instability induced by pure dilatation should have no difficulty in showing which is correct.

Figure 3 shows the simulation results for both compression and tension loadings at 500 K. One sees the internal pressure decreases monotonically with tension until the strain reaches a value of 1.058, at which point the pressure shows a sudden relief. Correspondingly, the energy at the critical strain shows a sudden drop. The static structure factor gives little indication of any structural change, while the mean squared displacement shows a dramatic increase in atomic displacement. Upon detailed examination of the atomic configurations after the unstable structural response, we find that cavitation has taken place in the previously homogeneous lattice. The sudden creation of a surface around the region of cavitation provides a mechanism to relieve some of the tension and lower the energy (by allowing particles to relax to a state of lower local stress). It also explains why the system apparently remained relatively ordered and indicates that the large mean square displacement is likely due to the opening of the cavity.

The clearcut conclusion from Fig. 3 is that the observed instability occurs at a critical strain, which agrees very closely with that predicted by the present stability criteria. Moreover, the symmetry associated with the onset of cavitation points to the vanishing of B_T rather than the vanishing of G'. Thus, by direct comparison we have demonstrated the validity of the present stability criteria, and at the same time the inapplicability of the conventional criteria.

Results corresponding to those given in Figs. 2 and 3 also have been obtained at several other temperatures: 200, 800, 1000, and 1200 K. Figure 4 shows the strain at which each stability criterion is violated as given by (4.4)–(4.6). At each temperature, therefore, the predicted critical strain is again the lowest value of strain at which the first violation occurs. Figure 4 also shows the observed values from the direct simulation. It is seen that the predictions agree well with the simulation results. Notice that while at 800 K instability occurs when the bulk modulus vanishes, a crossover from decohesion to tetragonal shear takes place at still higher temperature, such that at 1200 K the mechanism of unstable structural response is now clearly the vanishing of G'.

Returning to the question of what is the structural state of the system after the onset of instability, we note that the instability at 800 K is accompanied by a potential energy increase and an abrupt vanishing of the static structure factor, as shown in Fig. 5. This characteristic behavior is indicative of loss of crystalline order. Indeed, inspection of the atomic configurations generated during the simulation shows that the lattice has become completely disordered. The disordering, brought on by the spinodal instability, stands in distinct contrast to the structural response previously observed at 500 K, where at the onset of spinodal instability the potential energy decreased and $S(k)$ shows little change (cf. Fig. 3). As we reported earlier, in the latter case the atomic configurations revealed the formation of a cavity with the remaining lattice still reasonably well ordered.

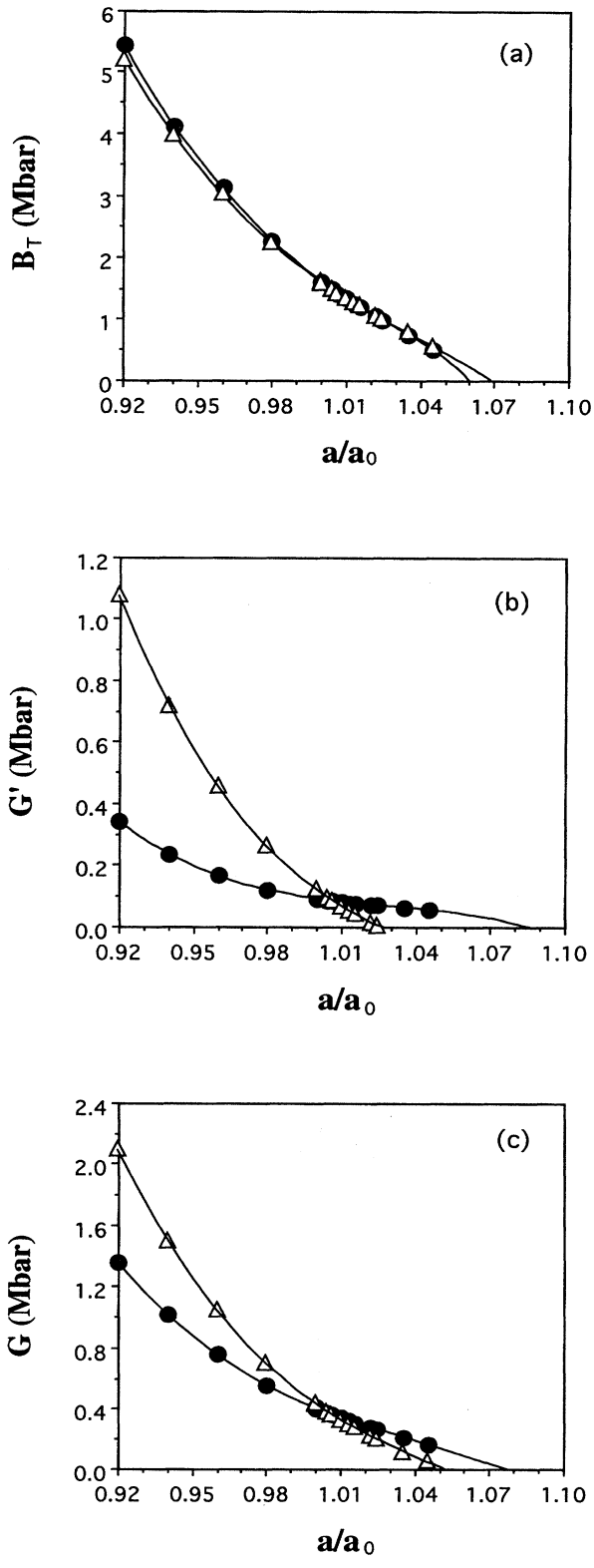

FIG. 2. Variations with hydrostatic strain of moduli associated with elastic stiffness coefficients (4.4)–(4.6) (closed symbols) and with elastic constants (4.1)–(4.3) (open symbols), respectively, (a) bulk modulus, (b) tetragonal shear modulus and (c) rhombohedral shear modulus. Lines show low-order polynomial fits to the data points.

V. DISCUSSION

In this work we have analyzed the stability of a homogeneous lattice under a constant uniform load by formulating a Gibbs integral which combines the change in the Helmholtz free energy with the work done by the applied stress. Because it is dependent on the path of deformation, this integral cannot be used directly to assess stability in the sense of a true thermodynamic potential. We showed that the integrand of the Gibbs integral leads to an effective force field acting in the deformation space; moreover, this quantity is characterized by the elastic stiffness tensor as defined in (2.21). Using the fact that the force field provides a direction for action, we arrive at a condition for instability involving the symmetrized form of the stiffness tensor (2.26).

We demonstrate that this approach provides an accurate means of predicting the maximum deformation (strain) that the lattice can sustain before the system becomes structurally unstable, the simple test being a comparison with direct molecular-dynamics simulation. In verifying (3.3)–(3.5), we show at the same time that the conventional criteria attributed to Born, obtained by setting $P=0$ in (3.3)–(3.5), are not valid at finite load, a limitation which appears not to have been fully recognized in previous studies of ideal strengths of solids.[3–5] It should be noted here that the technique developed by Parrinello and Rahman[13] for carrying out simulation at constant stress is ideally suited to the present purpose, since it corresponds precisely to the conditions under which the derivation is made. Direct simulation therefore provides the cleanest test of the theoretical limits of lattice stability.

It is noteworthy that the present stability analysis, based on only elasticity considerations, turns out to describe so accurately the onset of structural instability observed by atomistic simulations. This correspondence provides not only a method for the determination of ideal strengths at finite temperatures, but also an approach to understanding the role of elastic stability in various structural transitions such as stress-induced polymorphism and amorphization, and homogeneous melting. While stability analysis itself is incapable of determining the final configuration to which a structurally unstable system will evolve, it is an invaluable aid in the interpretation of molecular-dynamics simulations.

In several current studies, (2.22) has led to precise identifications of the elastic instability which triggers the structural transition. In hydrostatic compression of Si in the diamond cubic structure, the instability which causes the transition to β-tin structure is found to be the vanishing of the tetragonal shear $G'(P)$.[17] In contrast, compression of crystalline SiC in the zinc blende structure results in an amorphization transition associated with the vanishing of $G(P)$.[18] For behavior under tension, crack nucleation in SiC (Ref. 19) and cavitation in a model binary intermetallic,[20] both triggered by the spinodal instability, the vanishing of $B_T(P)$, are results which are analogous to the observations reported here. Notice, however, that in the present work a crossover at high temperature from spinodal to shear instability takes place. Further studies using the present EAM potential model have been made. While the detailed results will be reported elsewhere, it is pertinent to mention here that under uniaxial tension a transition from fcc to bcc was observed at the instability where $G'(P)$ vanished. The prob-

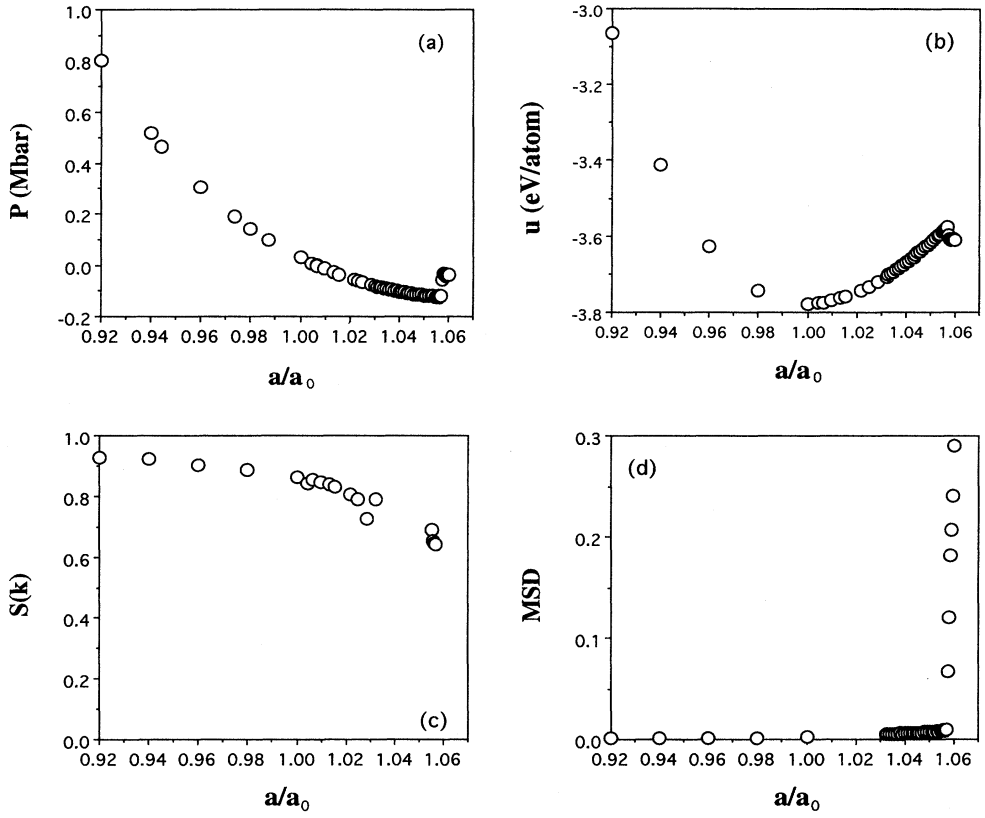

FIG. 3. Overall system responses at 500 K to hydrostatic strain, internal pressure P (a), potential energy per atom u (b), static structure factor $S(k)$ (c), and mean squared displacement MSD (d), all showing an instability at a critical strain of about 1.06.

lem of isobaric heating at zero pressure is of particular interest because then there is no difference between the present stability criteria and those due to Born. We found that the homogeneous lattice melts at the onset of instability again associated with the vanishing of $G'(P)$.[21]

Present work shows clearly the connection between the stability criteria for a crystal under load, our (2.26) and the more approximate result (2.29), and the well-known stability criteria, generally attributed to Born, $\det|C|=0$. One sees immediately that the latter conditions are valid only for a crystal under no external load. The distinction between the fourth-rank tensor B, which we call the elastic stiffness coefficient, and the second-order elastic constant tensor C is apparent from (2.22). This is a central relation in our analysis. While it has been derived previously,[14,22] its essential role in the determination of lattice stability under load apparently has not been recognized in the way we have presented here. It is worth noting that it is intuitively reasonable that stability criteria for crystals under load should depend explicitly on the loading. As (2.22) shows, the effect of the external work, to the order of our analysis, appears as a group of terms involving only the applied stress. Since the symmetry of the group depends only on the loading and therefore is unrelated to the symmetry of lattice, B has mixed symmetry. If we regard B as the tensor of effective elastic moduli, then according to (2.29) the condition for stability is not a question of intrinsic material property alone. We also note that in general B does not have Voigt symmetry, $B_{ijkl}=B_{klij}$, and that it does not satisfy Cauchy relations, $B_{ijkl}=B_{ikjl}=\ldots$.[6,23]

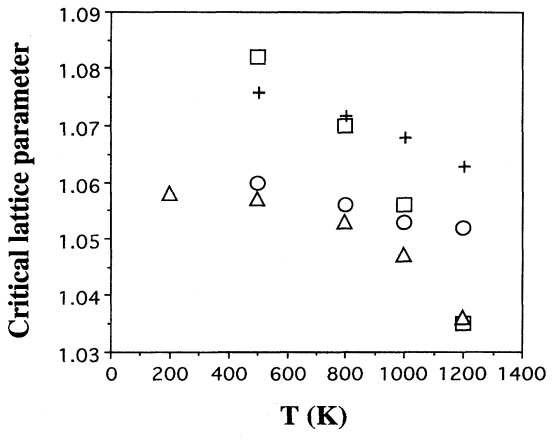

FIG. 4. Variation of critical strain with temperature of EAM (Au) model under hydrostatic tension; predictions based on (4.4)–(4.6) are denoted by circles, squares, and crosses, respectively. Strains at which instability occurred in simulation are indicated by triangles.

We are not aware of any previous derivation of (2.26) and (2.29). On the other hand, Hill and Milstein[7] have written down a formal expression combining the strain energy and the external work which is equivalent to (2.13) and derived stability criteria under volumetric deformation for different

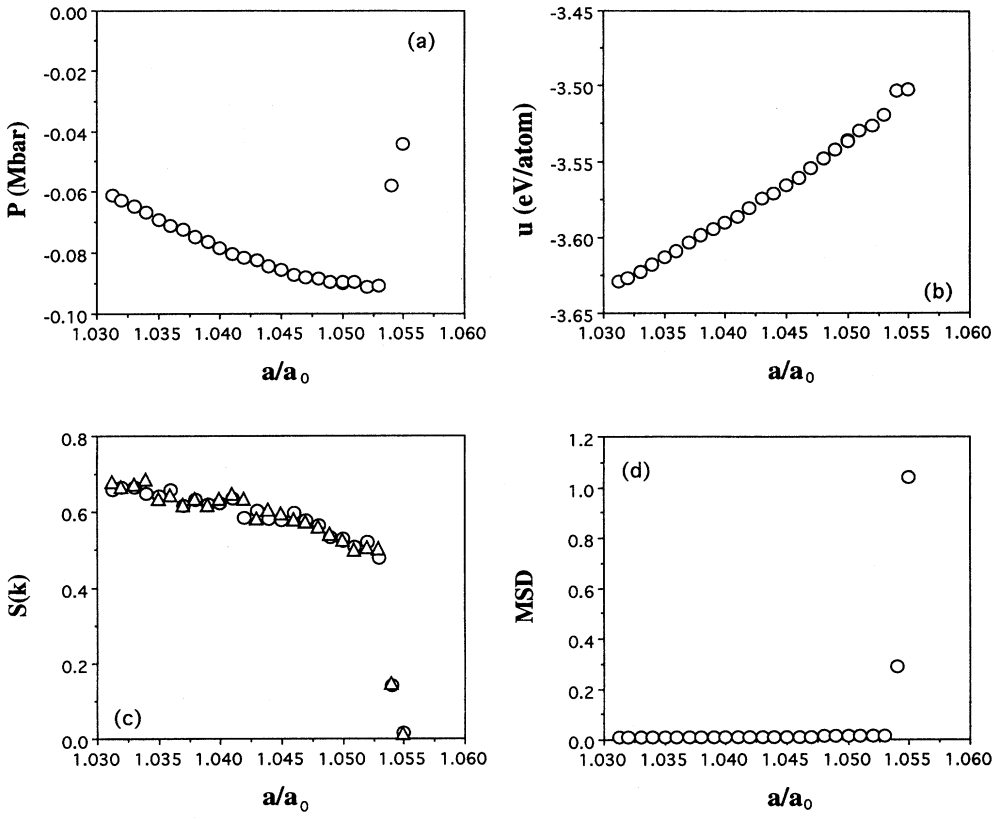

FIG. 5. Same as Fig. 3 except at 800 K. Note the increase in potential energy and vanishing of the static structure factor at the onset of instability, in contrast to Fig. 3. In addition, magnitude of MSD is much greater.

choices of strain measure. Our stability criteria based on (4. 4)–(4.6) agree identically with their results[7] for the case of Green's strain measure. For a summary of the series of studies on crystal stability under load and the relativity of the Born criteria carried out by Hill and Milstein, one should see the review of Milstein.[24]

Finally, we note that the disordering of a homogeneous lattice under isobaric heating at zero pressure can be regarded as an unstable structural response triggered by an elastic instability. In this case, the appropriate stability criteria are those given by Born. Through a combination of stability analysis and direct molecular-dynamics simulation, one can show that the thermoelastic concept of melting proposed by Born[25] and later extended by Boyer[26] indeed holds, provided heterogeneous nucleation is suppressed by the elimination of all defects.[21]

ACKNOWLEDGMENTS

One of us (S.Y.) would like to acknowledge discussions with F. Milstein concerning the work of Hill and Milstein. The work of J.W. and S.Y. has been supported in part by NSF (Grant No. CHE-8806767), AFOSR (Grant No. 91-0285), ONR (Grant No. N00014-92-J-1957), and the Materials Science Division, Argonne National Laboratory. Acknowledgment is made to the donors of The Petroleum Research Fund, administered by the ACS, for partial support of this research. J. W. also acknowledges support from the C. C. Wu Foundation. The work of S.R.P. and D.W. is supported by the U.S. Department of Energy, BES Materials Science, under Contract No. W-31-109-Eng-38. Computations were carried out in part under allocations from the San Diego Supercomputer Center and from the Lawrence Livermore National Laboratory.

[1] M. Born, Proc. Cambridge Philos. Soc. **36**, 160 (1940).
[2] M. Born and K. Huang, *Dynamical Theory of Crystal Lattices* (Clarendon, Oxford, 1956).
[3] M. Born and R. Furth, Proc. Cambridge Philos. Soc. **36**, 454 (1940).
[4] F. Milstein, Phys. Rev. B **3**, 1130 (1971); J. Appl. Phys. **44**, 3833 (1973).
[5] N. H. Macmillan and A. Kelly, Proc. R. Soc. London A **330**, 291 (1972); **330**, 309 (1972).
[6] R. Hill, Math. Proc. Cambridge Philos Soc. **77**, 225 (1975).
[7] R. Hill and F. Milstein, Phys. Rev. B **15**, 3087 (1977).
[8] F. Milstein and R. Hill, Phys Rev. Lett. **43**, 1411 (1979).
[9] F. Milstein and R. Hill, J. Mech. Phys. Solids **25**, 457 (1977).
[10] F. Milstein and R. Hill, J. Mech. Phys. Solids **26**, 213 (1978).
[11] F. Milstein, in *Mechanics of Solids*, edited by H. G. Hopkins and M. J. Sewell (Pergamon, Oxford, 1982), p. 417.
[12] F. D. Murnaghan, *Finite Deformation of an Elastic Solid* (Wiley, New York, 1950).

[13] M. Parrinello and A. Rahman, J. Appl. Phys. **52**, 7182 (1981).
[14] D. C. Wallace, *Thermodynamics of Crystals* (Wiley, New York, 1972).
[15] S. Foiles, M. I. Baskes, and M. S. Daw, Phys. Rev. B **33**, 7983 (1986).
[16] J. Ray, Comput. Phys. Rep **8**, 109 (1988).
[17] K. Mizushima, S. Yip, and E. Kaxiras, Phys. Rev. B **50**, 14 952 (1994).
[18] M. Tang and S. Yip, Phys. Rev. Lett. (to be published).
[19] M. Tang and S. Yip, J. Appl. Phys. **76**, 2719 (1994).
[20] F. Cleri, J. Wang, and S. Yip, J. Appl. Phys. **77**, 1449 (1995).
[21] J. Wang, S. Yip, S. Phillpot, and D. Wolf, Phys. Rev. Lett **77**, 4182 (1993).
[22] T. H. K. Barrons and M. L. Klein, Proc. Phys. Soc. **85**, 523 (1965).
[23] In an analysis of Cauchy relations, I. Stakgold [Quant. Appl. Math. **8**, 169 (1950)] has pointed out an inconsistency in Born's derivations. This has also been quoted by Hill in Ref. 6. For earlier discussions of Cauchy relations, see P. S. Epstein, Phys. Rev. **70**, 915 (1946); C. Zener, Phys. Rev. **71**, 323 (1947).
[24] F. Milstein, J. Mater. Sci. **16**, 1071 (1980).
[25] M. Born, J. Chem. Phys. **7**, 591 (1939).
[26] L. Boyer, Phase Transitions **5**, 1 (1985).